

Predicting proton-nucleus total reaction cross sections up to 300 MeV using a simple functional form

P. K. Deb* and K. Amos†

School of Physics, The University of Melbourne, Victoria 3010, Australia

(Dated: November 1, 2018)

Abstract

Total reaction cross sections are predicted for proton scattering from various nuclei. A simple functional form has been used that reproduces the total reaction cross sections for the scattering of protons from (15) nuclei spanning the mass range from ${}^9\text{Be}$ to ${}^{238}\text{U}$ and for proton energies 10 to 300 MeV.

PACS numbers: 25.40.-h,24.10.Ht,21.60.Cs

arXiv:nucl-th/0212051v1 12 Dec 2002

*Electronic address: pkd@physics.unimelb.edu.au

†Electronic address: amos@physics.unimelb.edu.au

I. INTRODUCTION

Reaction cross sections from the scattering of nucleons by nuclei (stable and radioactive) are required in a number of fields of study; some being of quite current interest [1]. Those fields range from problems in basic science through many of applied nature. An example of the latter is the transmutation of long lived radioactive waste into shorter lived products using accelerator driven systems (ADS). As well, proton-nucleus (p - A) cross section values at energies to 300 MeV or more are needed not only to specify important quantities of relevance to proton radiation therapy [2], but also as they are key information in assessing radiation protection for patients. As an example in basic science, total reaction cross sections are important ingredients to a number of problems in astrophysics. Also the integral observable of proton scattering from a given nucleus gives direct information on the neutron root mean square radius in nuclei [3]; a property sought in parity-violating electron scattering experiments [4].

It would be very utilitarian if aspects of such scattering were well approximated by a simple convenient functional form. Recently it has been shown [8] that, for neutron total reaction cross sections, such a form may exist. Herein we consider that concept further to reproduce the measured total reaction cross sections from proton scattering for energies ranging from 10 MeV to 300 MeV, and from 15 nuclei ranging in mass from 9 to 238.

II. FORMALISM

The total reaction cross sections for proton scattering from nuclei can be expressed in terms of partial wave scattering (S) matrices specified at energies $E \propto k^2$, by

$$S_l^\pm \equiv S_l^\pm(k) = e^{2i\delta_l^\pm(k)} = \eta_l^\pm(k) e^{2i\Re[\delta_l^\pm(k)]} , \quad (1)$$

where $\delta_l^\pm(k)$ are the (complex) scattering phase shifts and $\eta_l^\pm(k)$ are the moduli of the S matrices. The superscript designates $j = l \pm 1/2$. Total reaction cross sections then follow from

$$\begin{aligned} \sigma_R(E) &= \frac{\pi}{k^2} \sum_{l=0}^{\infty} \left\{ (l+1) \left[1 - (\eta_l^+)^2 \right] + l \left[1 - (\eta_l^-)^2 \right] \right\} \\ &= \frac{\pi}{k^2} \sum_{l=0}^{\infty} \sigma_l^{(R)}(E) . \end{aligned} \quad (2)$$

Despite the successes with use of the g -folding approach to define NA optical potentials [6], we note that there are discrepancies between the predictions of total reaction cross sections found thereby and actual data. Those usually are due to limitations with the structure model used to describe the ground state densities of some nuclei. However, there have been so many successes with the approach [1, 5, 6, 7] that we believe the functional form developed here on the basis of matching the values obtained with g -folding potentials are pertinent initial guesses to start a refinement (of the parameter values) to reproduce actual measured total reaction cross sections.

As evident from the figures presented in a recent paper [8], the partial total reaction cross sections, $\sigma_l^{(R)}(E)$, can be described by the simple functional form,

$$\sigma_l^{(R)}(E) = (2l+1) \left[1 + e^{\frac{(l-l_0)}{a}} \right]^{-1} + \epsilon(2l_0+1) e^{\frac{(l-l_0)}{a}} \left[1 + e^{\frac{(l-l_0)}{a}} \right]^{-2} \quad (3)$$

with $l_0(E, A)$, $a(E, A)$, and $\epsilon(E, A)$ varying smoothly with energy and mass.

The summation giving the total reaction cross section can be limited to a value l_{max} and the associated form tends appropriately to the known high energy limit. With increasing energy, l_{max} becomes so large that the exponential fall of the functional form, Eq. 3, can be approximated as a straight vertical line ($l_0 = l_{max}$). In that case, the total reaction cross section equates to the area of a triangle, and

$$\sigma_R \Rightarrow \frac{\pi}{2k^2} l_{max} (2l_{max} + 1) \approx \frac{\pi}{k^2} l_{max}^2 . \quad (4)$$

Then with $l_{max} \sim kR$, at high energies

$$\sigma_R \Rightarrow \pi R^2 ; \quad (5)$$

the geometric cross section as required.

III. RESULTS AND DISCUSSIONS

Although on using Eqs. 2 and 3 to match values of (theoretically) calculated total reaction cross sections led [8] to the three parameters $l_0(E, A)$, $a(E, A)$, and $\epsilon(E, A)$ having smooth variations with energy, there are discrepancies between those predictions and the actual measured data. Herein we modify the method of selection of those parameter values to produce more accurate reaction cross section values, while keeping as smooth a variation with energy of those parameters as possible. Specifically, in Eq. 3, we have set the ϵ as a constant (-1.5) and so independent of energy and of mass. Further we assume that $a(E, A)$ varies linearly with the wave vector,

$$k = \frac{1}{\hbar c} \sqrt{E^2 - m^2 c^4} , \quad (6)$$

and with the form

$$a(E, A) \sim 1.02k - 0.25 . \quad (7)$$

Then $l_0(E, A)$ were adjusted to ensure that all measured total reaction cross section values are matched by using the function form, Eq. 3.

The resultant optimized values for the parameter l_0 are presented in Fig. 1. In this figure, the points represent the calculated values of l_0 at particular energies where the experimental values of total reaction cross sections are available for the considered nuclei. We have used the lower and upper uncertainty limits to get the error bars for l_0 values. We call these l_0 values with uncertainties as "data- l_0 " hereafter. The curves result on using a spline interpolation on those data points constrained to give an optimal smoothness variation of $l_0(E, A)$ with E. The figure displays the results for the entire energy range (to 300 MeV) in the left hand panels, while the right hand panels emphasize the low energy variations to 50 MeV since most experimental values lie in that range of energy.

In panel (a) of Fig. 1, the solid, dotted, dashed, long-dashed, and dot-dashed lines depict the values for ^9Be , ^{12}C , ^{16}O , ^{19}F , and ^{27}Al respectively, as do circles, squares, diamonds, up triangles and down triangles for the data- l_0 results. The same legends apply to the 10 to 50 MeV plots shown in panel (b). In panels (c) and (d), the energy variations of l_0 values for ^{40}Ca , ^{63}Cu , ^{90}Zr , ^{118}Sn , and ^{140}Ce are presented by solid, dotted, dashed, long-dashed and dot-dashed lines respectively. The corresponding data- l_0 points are also presented by

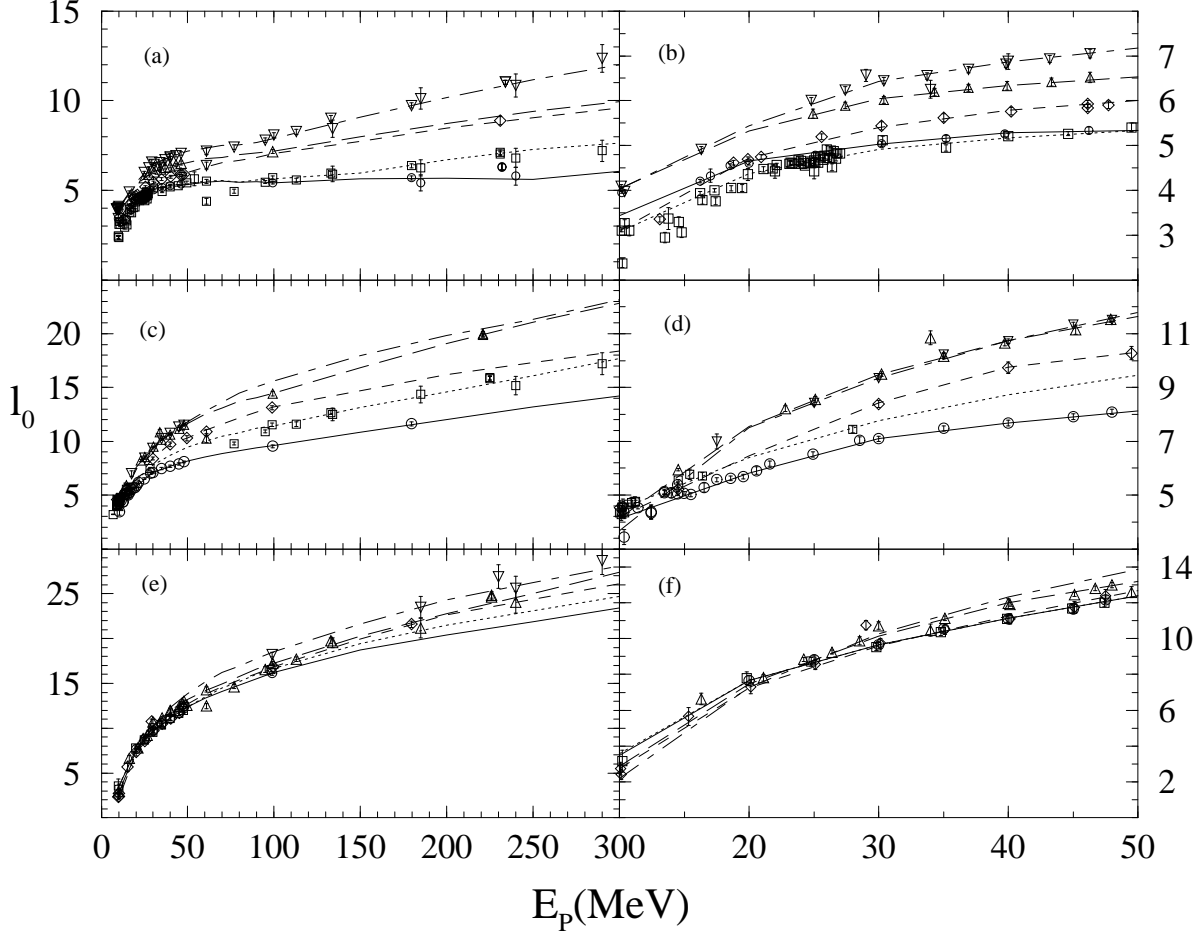


FIG. 1: The parameter values for l_0 in the simple functional form for the p - A reaction cross sections. Points shown with error bars are the values required to match actual measured data values.

circles, squares, diamonds, up triangles and down triangles. Finally, in panels (e) and (f), we display the variations of l_0 with energy for ^{159}Tb , ^{181}Ta , ^{197}Au , ^{208}Pb and ^{238}U by solid, dotted, dashed, long-dashed and dot-dashed lines respectively with the corresponding data- l_0 points presented by circles, squares, diamonds, up triangles and down triangles.

Numerical values for l_0 that result from the simple functional form calculations and as displayed by the curves in Fig. 1, are listed at various energies in Table. I. For energies 50 MeV and higher, these l_0 values monotonically increase with mass and energy as might be anticipated. At lower energies however, and while the l_0 values do still vary monotonically with energy, there is structure in their mass variation. In particular, the values of l_0 for ^{197}Au , ^{208}Pb and ^{238}U in the energy range from 10 MeV to 20 MeV decrease with mass. But note that there is little data available for these nuclei at this energy range.

The mass variations given by these tabled values have extra structure as is evident from the plots given in Fig. 2. The results are not as smooth as the counterpart variation with energy particularly at the lowest of the energy set. That may reflect the scattered (in energy) nature of the actual data from which starting values of l_0 have been taken to generate the functional forms.

In Figs. 3, 4, and 5, we show the total reaction cross sections generated using the simple functional form and tabled values of l_0 , and displayed by the solid curves, with

TABLE I: l_0 values for different nuclei at different energies.

Energy (MeV)	Nucleus														
	^9Be	^{12}C	^{16}O	^{19}F	^{27}Al	^{40}Ca	^{63}Cu	^{90}Zr	^{118}Sn	^{140}Ce	^{159}Tb	^{181}Ta	^{197}Au	^{208}Pb	^{238}U
10	3.43	3.08	3.11	4.04	4.02	4.12	4.47	4.18	4.15	3.67	3.47	3.57	2.75	2.87	2.19
20	4.65	4.37	4.72	5.32	5.44	5.82	6.40	6.46	7.56	7.51	7.65	7.66	7.24	7.45	7.28
30	5.03	4.91	5.40	6.04	6.43	7.09	7.77	8.42	9.47	9.36	9.67	9.65	9.60	10.14	10.26
40	5.29	5.17	5.78	6.34	6.86	7.69	8.73	9.76	10.74	10.75	11.13	11.13	11.25	11.99	12.31
50	5.34	5.34	6.00	6.53	7.17	8.14	9.46	10.31	11.64	11.79	12.37	12.38	12.68	13.19	13.87
60	5.44	5.50	6.28	6.75	7.35	8.56	10.01	10.98	12.50	12.76	13.34	13.48	13.75	14.18	15.15
70	5.51	5.54	6.53	6.83	7.49	8.88	10.46	11.60	13.10	13.65	14.12	14.47	14.61	14.94	16.22
80	5.46	5.45	6.66	7.00	7.52	9.13	10.80	12.16	13.76	14.46	14.83	15.22	15.41	15.76	16.90
90	5.48	5.57	6.85	7.08	7.66	9.38	11.19	12.71	14.04	15.06	15.53	16.02	16.09	16.59	17.79
100	5.42	5.64	7.05	7.19	7.88	9.63	11.44	13.20	14.48	15.61	16.21	16.64	16.88	17.25	18.51
150	5.63	5.97	7.72	7.98	9.09	10.87	13.14	14.70	16.82	17.95	18.71	19.41	19.92	20.25	21.65
200	5.65	6.70	8.47	8.73	10.17	12.04	14.58	16.18	19.08	19.86	20.68	21.50	22.23	22.75	24.34
250	5.61	7.29	9.06	9.39	11.15	13.17	16.12	17.90	20.19	21.33	22.38	23.65	24.40	25.01	26.24
300	6.07	7.64	9.58	9.96	12.01	14.23	17.22	20.05	22.37	23.79	24.70	25.91	26.90	27.41	28.11

those obtained from calculations made using g -folding optical potentials [5]. Dashed lines represent the predictions obtained from those microscopic optical model calculations. The experimental data [9] are depicted by circles.

The results for scattering from ^9Be , ^{12}C , ^{16}O , ^{19}F , ^{27}Al , and ^{40}Ca are displayed in segments (a) through (f) of Fig. 3 respectively. In segment (a), the data are well reproduced by the g -folding predictions resulting from the folding with the ^9Be ground state OBDME found with $(0+2)\hbar\omega$ spectroscopy as well as by those obtained with the simple functional form method.

Calculated p - ^{12}C reaction cross sections are compared with the experimental data in segment (b) of Fig. 3. The reaction cross sections obtained from g -folding calculations are in good agreement with the experimental data but only in the energy range above 20 MeV. On the other hand, the results obtained from the simple functional method are excellent for all energies, replicating the average trend of data well even in the lower energy range from 10 MeV. There are two data points, at 61 MeV and at 77 MeV, in disagreement with the calculated results however. But, as noted previously [1], these data points should be discounted.

Predictions for p - ^{16}O and for p - ^{19}F scattering are compared with data in segments (c) and (d) of Fig. 3. For p - ^{16}O case, there are many data points at the energies between 20 to 40 MeV. Predictions from g -folding calculations while replicating the data well at and above 25 MeV, overestimate at lower energies. That g -folding result also underestimates the datum at 250 MeV; the sole datum above 50 MeV. In contrast, and by design, the results obtained from the simple functional method are in excellent agreement with the experimental data at all energies. For p - ^{19}F , although g -folding calculations reproduce the data well, the simple functional form method gives slightly more accurate predictions.

Total reaction cross section predictions for p - ^{27}Al and for p - ^{40}Ca are compared with the experimental data in segments (f) and (g) of Fig. 3. Again while g -folding calculations

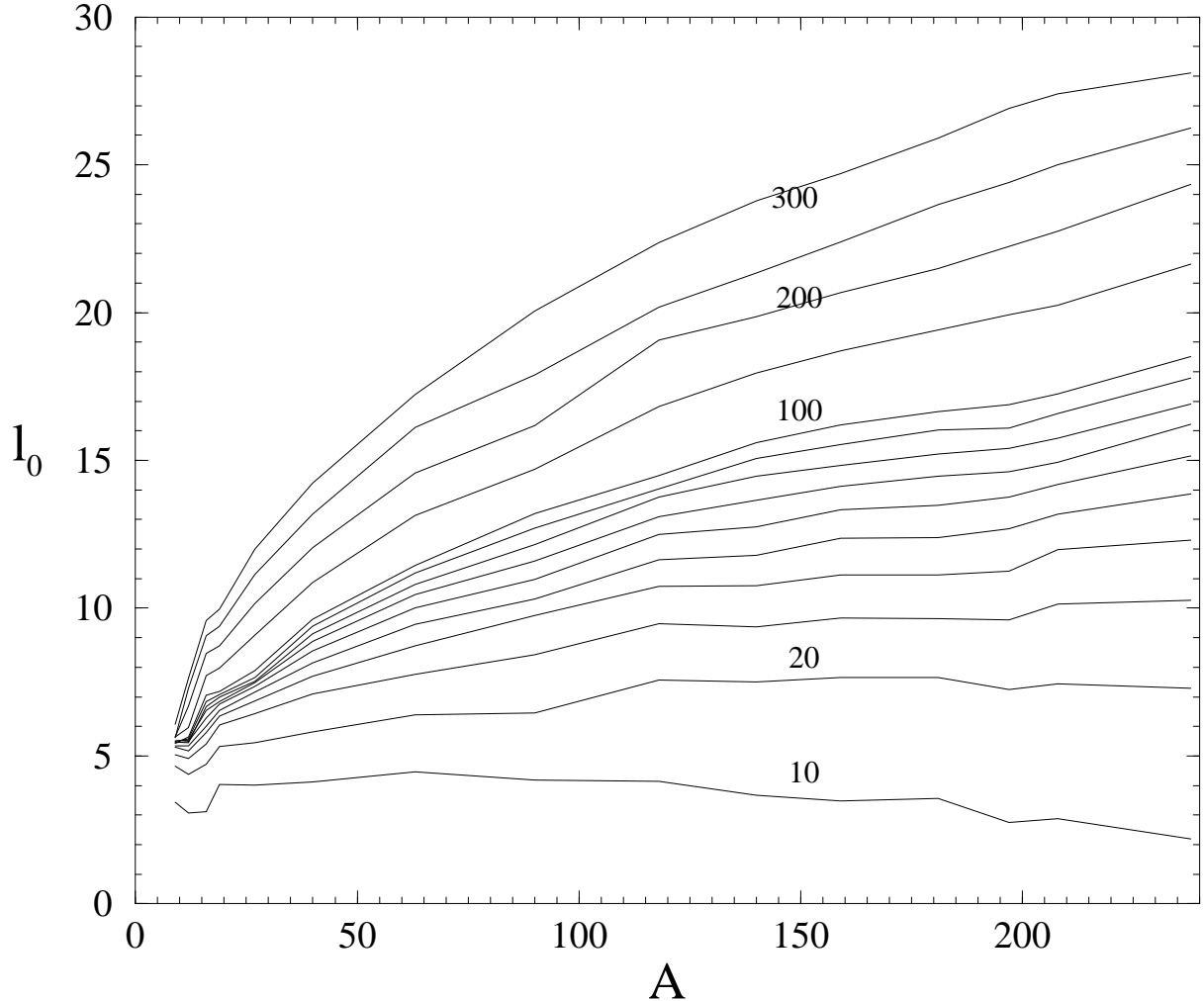


FIG. 2: The parameter values for l_0 in the simple functional form for the p - A reaction cross sections as a function of target mass for each energy given in the table.

reproduce the data quite well to 200 MeV, three data points between 180 and 300 MeV are not matched. The g -folding results underestimate them noticeably. But predictions from a simple functional form approach replicate the data well at all energies. One data point at 61 MeV is exceptional in the set. With ^{40}Ca , the folding model approach is not expected to be reliable at the energies in the range 10 to 20 MeV, as is the case with ^{12}C , since for excitation energies of that range, both nuclei have clearly discrete spectra. That is true for most light mass nuclei but little or no total reaction cross sections have been reported for them. Indeed the reaction data from both ^{12}C and from ^{40}Ca show rather sharp resonance features below 20 MeV. Both the g -folding calculations and functional form calculations reproduce the rest of the ^{40}Ca data well.

The results for scattering from ^{63}Cu , ^{90}Zr , ^{118}Sn , ^{140}Ce , ^{159}Tb , and ^{181}Ta are displayed in Fig. 4 in segments (a) through (f) respectively. For ^{63}Cu , predictions at low energies may be slightly too small and the parameter sets driven too severely by the sole datum at 30 MeV

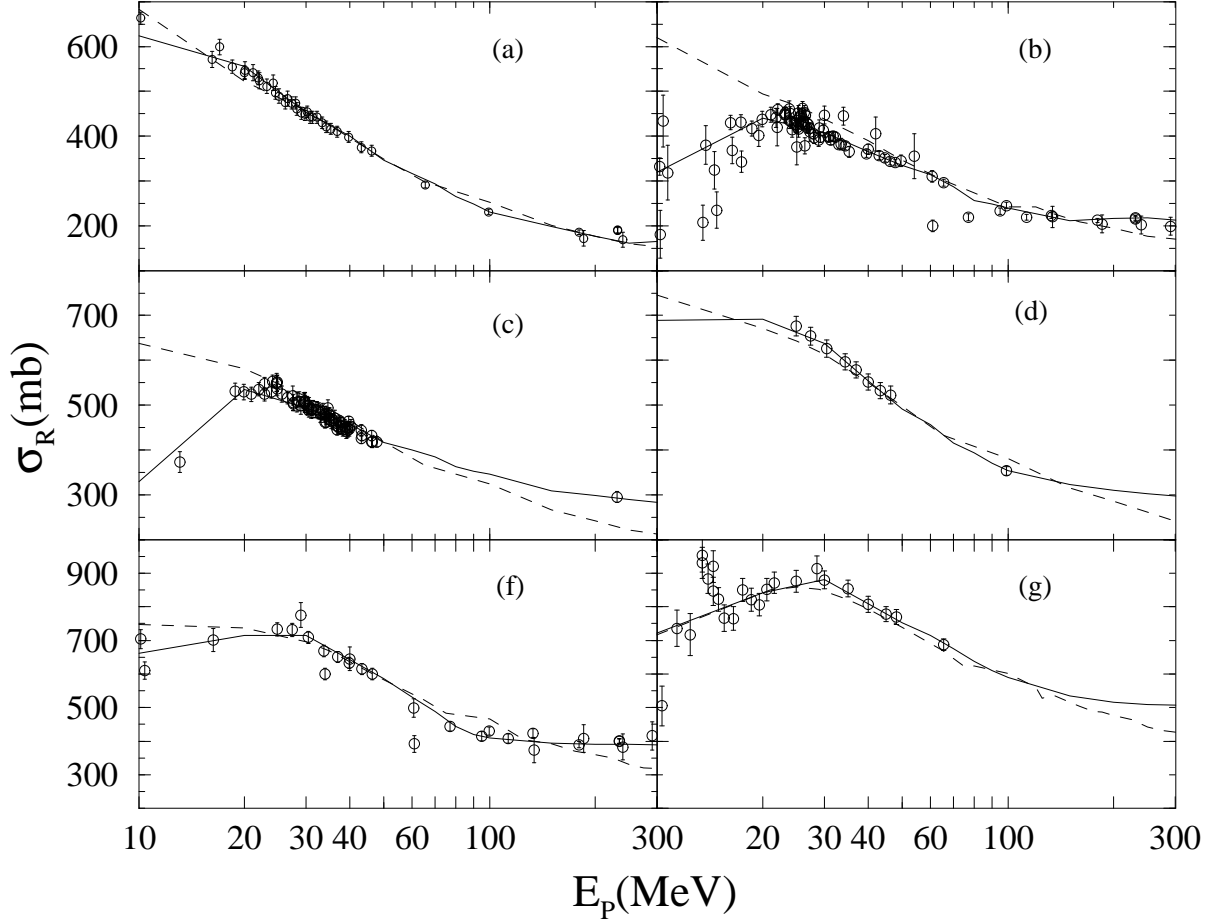


FIG. 3: Energy dependence of σ_R for proton scattering from (a) ^9Be , (b) ^{12}C , (c) ^{16}O , (d) ^{19}F , (e) ^{27}Al and (f) ^{40}Ca . Dashed lines represent the results obtained from g -folding optical potential calculations while the solid curves portray the values obtained by using simple functional form.

in the range 20 to 70 MeV. Also the data in the range 100 to 300 MeV are quite scattered but the simple functional form gives a good average result.

In segment (b) of Fig. 4, the predicted total reaction cross sections from p - ^{90}Zr scattering are compared with the experimental data. Results from g -folding calculations are in good agreement with the data although the data value at 30 MeV is overestimated. The results obtained from the simple functional form, and by dint of construction, are in excellent agreement with the experimental data at the few energies measured, but the shape is not optimally smooth. This we believe is the prime cause for the kink shown at $A = 90$ in the mass variation plots in Fig. 2 and most noticeably at 200 MeV. Lack of data meant that we had to use the g -folding values to specify the functional form. That is also the case with masses 140, 159, and 181.

The p - ^{118}Sn total reaction cross section results are given in segment (c) of Fig. 4 where the two predictions again are compared with the data. Although not as good as the results found for scattering from light mass nuclei, the g -folding potential still gives reasonable shape prediction. However, the model underestimates the data by 5 to 10%. But the simple functional form model form again gives an excellent reproduction of the data at all energies except 61 MeV. This 61 MeV data point is again exceptional being much smaller than other

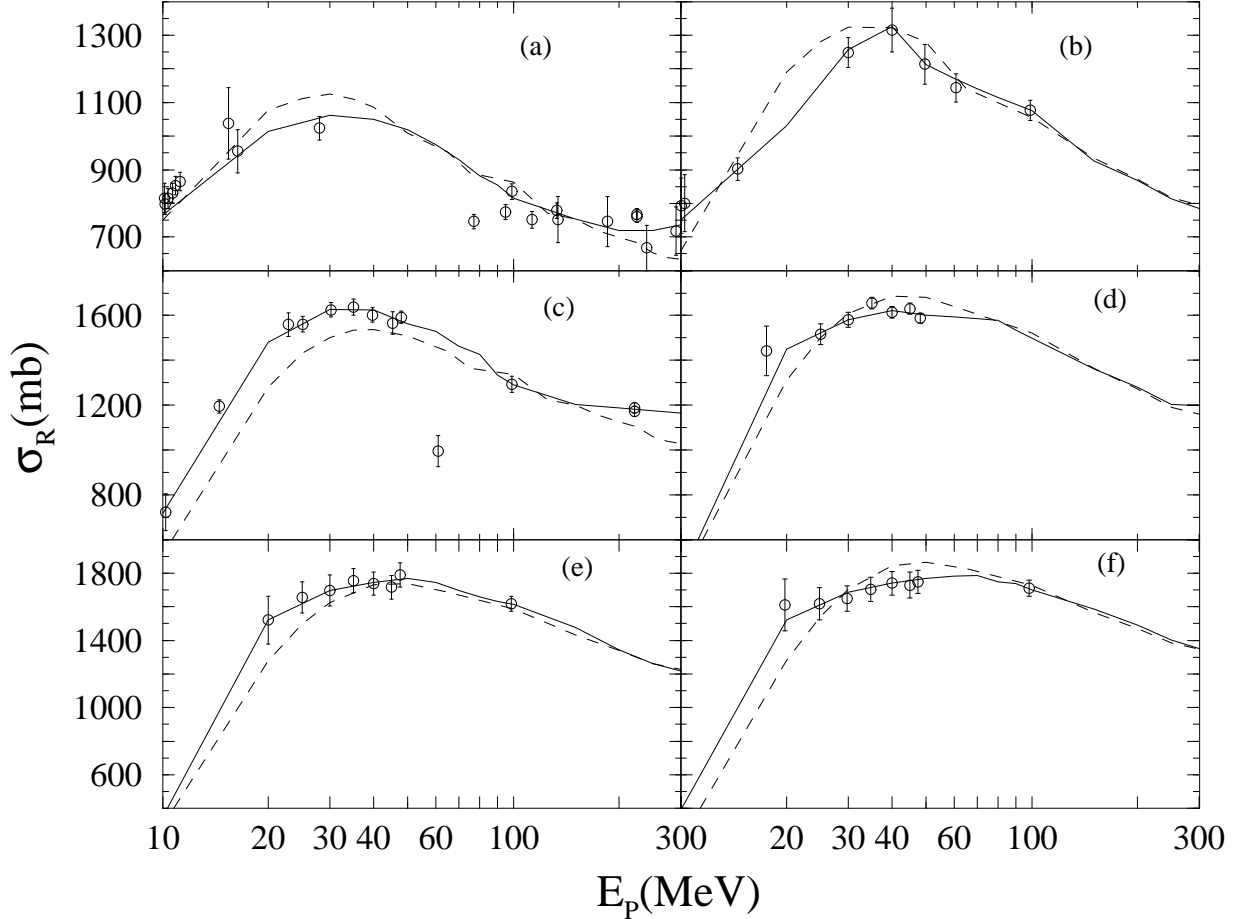


FIG. 4: Same as Fig. 3 but from (a) ^{63}Cu , (b) ^{90}Zr , (c) ^{118}Sn , (d) ^{140}Ce , (e) ^{159}Tb and (f) ^{181}Ta .

data and the predictions as in the cases of ^{12}C and ^{27}Al .

Predictions for $p\text{-}^{140}\text{Ce}$, $p\text{-}^{159}\text{Tb}$ and for $p\text{-}^{181}\text{Ta}$ scattering are compared with the (limited amount of) data in segments (d), (e) and (f) of Fig. 4 respectively. The g -folding calculations give good agreement with that data for $p\text{-}^{140}\text{Ce}$, slightly underestimate the data for $p\text{-}^{159}\text{Tb}$, and for $p\text{-}^{181}\text{Ta}$, underestimate data at the energies to 20 MeV and overestimate data in the energy range 40 to 60 MeV. In all cases results predicted by the simple functional form are excellent reproductions of the experimental data.

In segments (a), (b) and (c) of Fig. 5 we compare the calculated total reaction cross sections for $p\text{-}^{197}\text{Au}$, $p\text{-}^{208}\text{Pb}$ and $p\text{-}^{238}\text{U}$ scattering with the available data. For ^{197}Au , the g -folding optical potential calculations are in good agreement with most data; the 29 MeV datum grossly underestimated by the calculations. But that data point is also at odds with the energy trend of the other data. Save for that 29 MeV value, the simple functional form gives even better predictions of the data. The energy variation of the $p\text{-}^{208}\text{Pb}$ reaction cross sections is shown in segment (b) of Fig. 5 where the predictions from g -folding optical potential calculations and from the simple functional form calculations are compared with a fairly extensive set of experimental data. In making the g -folding potentials, we have used Skyrme-Hartree-Fock wave functions [3] which have been shown to be more realistic [5] than simple oscillator model ones. Still such g -folding calculations underestimate the data up to 50 MeV. But simple functional form calculations are in excellent agreement with the

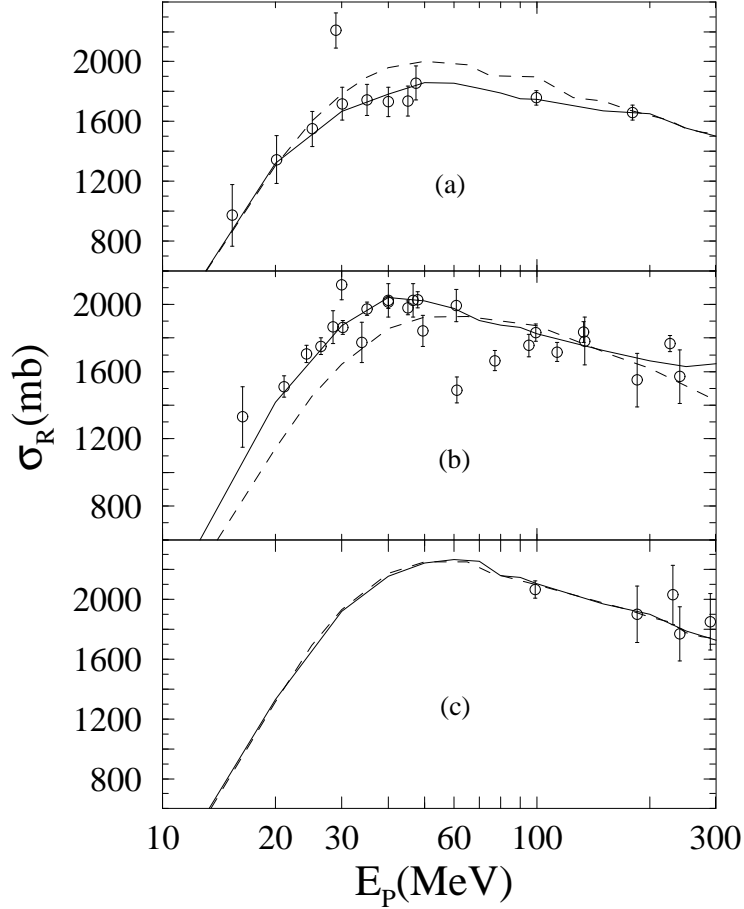


FIG. 5: Same as Fig. 3 but from (a) ^{197}Au , (b) ^{208}Pb , and (c) ^{238}U .

experimental data, save that data values at 30, 61 and 77 MeV again are exceptional. The predictions of total reaction cross sections for p- ^{238}U scattering from the g -folding optical potential calculations and from using the simple functional form are compared with the few data in segment (c) of Fig. 5. Given the lack of data the two results are virtually identical.

As a final note regarding many of the exceptional data values so defined in the foregoing, Menet *et al.* [10] argue that there may be a systematic error in the studies reported in those experiments.

IV. CONCLUSIONS

The measured reaction cross sections for 10–300 MeV proton scattering from nuclei ranging in mass from ^9Be to ^{238}U are well reproduced by calculations made using a three parameter function. The values of the parameters (l_0 , a , ϵ) are set in a simple manner and when set by enough actual data, can be used to predict the total reaction cross sections at any energy for a given nucleus. The mass variations of those parameters at fixed energies also are smooth, and very much so when data exists to control the results, and we believe that the simple functional form also can be used to find reasonable estimates of the total reaction cross sections of protons from any stable nucleus in the mass range.

Acknowledgments

This research was supported by a research grant from the Australian Research Council.

- [1] P. K. Deb, K. Amos, S. Karataglidis, M. B. Chadwick, and D. G. Madland Phys. Rev. Lett. **86**, 3248 (2001).
- [2] D. T. L. Jones, Acta Radiochim. **89**, 235 (2001).
- [3] B. A. Brown, Phys. Rev. Lett. **85**, 5296 (2000).
- [4] Jefferson Laboratory Experiment E-00-003, spokespersons R. Michaels, P. A. Souder, and G. M. Urciuoli.
- [5] K. Amos, S. Karataglidis, and P. K. Deb, Phys. Rev. C **63**, 064618 (32002).
- [6] K. Amos, P. J. Dortmans, H. V. von Geramb, S. Karataglidis, and J. Raynal, Adv. in Nucl. Phys. **25**, 275 (2000).
- [7] S. Karataglidis, K. Amos, B. A. Brown, and P. K. Deb, Phys. Rev. C **65**, 044306 (2002).
- [8] K. Amos and P. K. Deb, Phys. Rev. C **66**, 024604 (2002).
- [9] R. F. Carlson, At. Data Nucl. Data Tables **63**, 93 (1996).
- [10] J. J. H. Menet, E. E. Gross, J. J. Malanify, and A. Zucker, Phys. Rev. C **4**, 1114 (1971).